Distinguishing between primary and secondary emplacement events of blocky volcanic deposits using rock size distributions

M. H. Bulmer,[1] L. S. Glaze,[2] S. Anderson,[3] and K. M. Shockey[2]

Received 10 October 2003; revised 22 October 2004; accepted 27 October 2004; published 15 January 2005.

[1] Rock size characteristics in rock avalanches and blocky lava flows are different and statistical techniques can be used both to distinguish between and to constrain the different emplacement mechanisms of these two processes. At the Chaos Jumbles rock avalanche deposit in California, rock sizes decrease as a function of distance. The rock avalanche mechanism is an example of a secondary process that can only break existing blocks. In contrast, lava flows at Sabancaya, Peru, were emplaced by primary mechanisms capable of creating as well as breaking blocks. These deposits exhibit uniform block sizes as functions of distance and significantly larger blocks overall than Chaos Jumbles. Rock sizes at Inyo domes, also emplaced by a primary process, are significantly smaller in areas with compressional ridges as compared to vent or jumbled areas.

Citation: Bulmer, M. H., L. S. Glaze, S. Anderson, and K. M. Shockey (2005), Distinguishing between primary and secondary emplacement events of blocky volcanic deposits using rock size distributions, *J. Geophys. Res.*, *110*, B01201, doi:10.1029/2003JB002841.

1. Introduction

[2] A primary key to understanding past history of a volcano, and potentially future behavior, is interpretation of surface deposits. However, interpreting the origin of a blocky geologic surface is difficult, especially in instances where ground observations are not possible or where additional evidence that could provide spatial and temporal context for the deposit is ambiguous. This difficulty is compounded in volcanic terrains where lava flows and rock avalanches can occur in the same material and locality. Furthermore, postemplacement processes such as glaciation or fluvial activity may contribute additional complexity to interpreting the origin of a blocky surface. These problems are familiar to those working in mountainous and volcanic regions [e.g., *Eppler et al.*, 1987; *Gaddis et al.*, 1990], as well as to those interpreting remote data of the seafloor and of the terrestrial planets [e.g., *Moore et al.*, 1992; *Bulmer and Guest*, 1996; *Bulmer and Wilson*, 1999; *Stofan et al.*, 2000].

[3] Although several previous studies have investigated morphologic characteristics of lava flows and rock avalanches [e.g., *Fink*, 1983; *Eppler et al.*, 1987; *Fink and Manley*, 1987; *Fink and Griffiths*, 1990; *Fink et al.*, 1992; *Fink and Griffiths*, 1992; *Anderson and Fink*, 1992; *Anderson et al.*, 1995], relatively few have addressed surface rock size distributions. Those field studies that do address geologic rock size are often limited to qualitative discussions of angularity and sorting [*Udden*, 1914; *Wentworth*, 1922, 1935; *Tanner*, 1969; *Folk et al.*, 1970; *Blair and McPhearson*, 1999]. Where more quantitative data have been acquired, size information has been reduced to cumulative size-frequency distributions. For rock fields on Mars and in a number of geologic environments on Earth, these cumulative distributions typically exhibit an exponential form [e.g., *Malin*, 1988, 1989; *Golombek and Rapp*, 1997; *Anderson et al.*, 1998]. However, much of the detail contained in the raw measurement data is lost in this type of analysis. Here we demonstrate a field data collection technique that adequately estimates rock size populations from measurements. We also show that the individual sampling distributions can be used to distinguish between different emplacement processes that have statistically different rock size populations. This is significant in that conditions such as eruption rate, duration, velocity, and material rheology during emplacement can be assessed for events, such as lava flows and rock avalanches, that were unobserved. It therefore becomes possible, using high-resolution images of rocky surfaces on Earth and on planets such as Venus and Mars, to calculate rock size populations and obtain greater understanding of their emplacement histories.

[4] We investigate blocky surfaces on lava flows, lava domes and a rock avalanche from a collapsed lava dome. The lava flows discussed in this study are composed of dacitic and andesitic lavas. Lavas of these compositions typically erupt as domes and flows with the surfaces dominated by rocks that range from <5 cm to >6 m. While blocks are formed at the vent, they can be modified during flow by processes such as autobrecciation [*Cas and Wright*, 1987]. Blocks can also be added downslope through the exposure of cooled interior lava during compressional ridge

[1] Joint Center for Earth Systems Technology, University of Maryland, Baltimore County, Baltimore, Maryland, USA.
[2] Proxemy Research, Bowie, Maryland, USA.
[3] Geology and Planetary Science Department, Black Hill State University, Spearfish, South Dakota, USA.

Copyright 2005 by the American Geophysical Union.
0148-0227/05/2003JB002841$09.00

formation [*Anderson et al.*, 1998]. For the purposes of discussion, we refer to lava flow and dome emplacement as primary emplacement mechanisms.

[5] A rock avalanche from collapse of a lava dome primarily comprises blocks from the preavalanche dome that were broken during mass movement. The term avalanche relates to the kinematics of movement of the loose material involved rather than to any material type or transport and failure mechanism. An avalanche requires no interstitial medium (unlike a debris flow) and can develop by the sudden mobilization of slope forming materials because of the fall of an overhanging rock mass or a seismic shock [*Angeli et al.*, 1998]. An avalanche following mechanical collapse of an existing edifice (e.g., lava dome) is referred to here as a secondary emplacement mechanism. The fundamental distinction between primary and secondary processes is that secondary mechanisms can only break existing rocks, whereas primary mechanisms are capable of both creating and degrading rocks.

[6] Detailed measurements used here were collected by *Bulmer and Campbell* [1999] and *Bulmer et al.* [2002] for the Chaos Jumbles (United States) rock avalanches and a blocky lava flow at Sabancaya Volcano (Peru). Data include local and regional flow slope, estimated block sizes along longitudinal and transverse profiles, and flow thickness measurements. Rock size data for the Inyo domes and Medicine Lake Volcano (United States) are from *Anderson et al.* [1998] and were collected along profiles on the flow surface. Data were collected at multiple sites on each deposit.

2. Field Sites

2.1. Chaos Jumbles

[7] The Chaos Jumbles in Lassen Volcanic National Park (40°32′N, 121°32′W), California (Figure 1), originated from a volcanic dome that forms part of the Chaos Crags [*Clynne*, 1999]. The initial event of the eruptive sequence was the formation of a tuff cone followed by two pyroclastic flows. A series of domes then formed (primary process) which were also partially destroyed by pyroclastic events. The Jumbles (covering an area of 6.8 km^2) were formed from the cold collapse (secondary process) of a dome by rock avalanches. On the basis of tree growth and lichenometry [*Heath*, 1960], flow margins and rock characteristics [*Eppler et al.*, 1987], three deposits were identified. These have been designated as I, II, and III by *Eppler et al.* [1987], with I being the oldest. The time interval between events I, II, and III has been suggested as ranging from thousands of years to a single event [*Williams*, 1928; *Crandell et al.*, 1974; *Eppler et al.*, 1987; *Clynne*, 1999]. The deposits consist of a monolithologic breccia of Chaos Crags dacite blocks in a matrix of pulverized dacite. Well-defined large-scale folds, ridges and furrows can be identified on these deposits that are morphologically similar to those found on lava flows and domes at Sabancaya, Medicine Lake, and Inyo.

[8] Dimensional data discussed here have been obtained on deposits II and III. Estimated rock sizes revealed variations in rock characteristics consistent with the existence of more than one deposit within the boundary of unit III. Individual rock streams that clearly flowed as discrete, coherent events are discernable in the field and vary in width from 1 m to <30 m, but are consistently one rock thick.

2.2. Sabancaya Volcano

[9] Sabancaya Volcano (15.47°S, 71.51°W) lies within the high Puna plateau of Peru and forms a part of the Cordillera Occidental; a NW-SE trending mountain range with peaks over 6000 m. The volcano is part of a complex that consists of Nevado Ampato (6299 m) to the south and Hualca Hualca (6025 m) to the north. Sabancaya Volcano has two summit domes surrounded by 38 thick blocky lobate andesitic trachyandesitic flows (Figure 2). These thick (100 m or more) flows (primary process) have large-scale fold structures. The last eruptive event at Sabancaya in 1990 deposited ash up to 20 km away and minor, sporadic explosive activity continues to this day. Limited age dating, geochemical analysis, and small-scale, large-area mapping have been conducted on Sabancaya [*Bulmer et al.*, 1999], but no detailed geological history of the volcano has been compiled.

[10] On the basis of mapping from air photos, *Bulmer et al.* [1999] proposed that the lava flow field originated from Sabancaya, though some of the lobes on the western side of the volcano originated from nearby Ampato Volcano. Of the total number of flows within the flow field, 38% are <1 km in length, while 40% are between 2 and 4 km. Flows that traveled initially northwest were diverted by Holocene glacial moraines causing them to follow a course to the southwest. Similarly, flows from Sabancaya that moved north were constrained by the break of slope at the southern flanks of a nearby volcano. Flows to the northeast also appear to have had their paths influenced by a break in slope. The longest flows traveled to the southeast, corresponding to the location of more open topography. The spread of these flows laterally was constrained only by the conditions within the flow at the time of emplacement. The flow surfaces at Sabancaya are characterized by large (>6 m) blocks. These blocks tend to be angular, making the flow appear similar to a blocky basaltic andesite flow, except for the large block size. The blocks are sufficiently large that this flow surface actually appears smooth at radar wavelengths <60 cm [*Bulmer et al.*, 2001].

[11] Rock populations discussed here have been obtained on flows 1 and 2a. Flow 2a is 3.5 km long and has flow margin and flow front slopes of 36°–38°. In the distal zone the flow is 108 m thick.

2.3. Inyo and Medicine Lake Volcano

[12] The youngest domes at Inyo are Deadman, Glass Creek, Obsidian, and Wilson Butte. They cut across the northern margin of Long Valley caldera in eastern California. Deadman, Glass Creek, and Obsidian domes are composed of a finely and coarsely porphyritic rhyolite [*Bailey et al.*, 1976]. Wilson Butte consists of a phenocryst-poor rhyolite [*Anderson et al.*, 1998]. At Medicine Lake Volcano, also in California, dacite and rhyolite extrusions include Glass Mountain, the Medicine Lake dacite flow, and the Crater Glass flows. Unlike Sabancaya, the flows at Medicine Lake have large vitreous and vesicular blocks [*Anderson et al.*, 1998]. The locations where rock size data for the Inyo domes

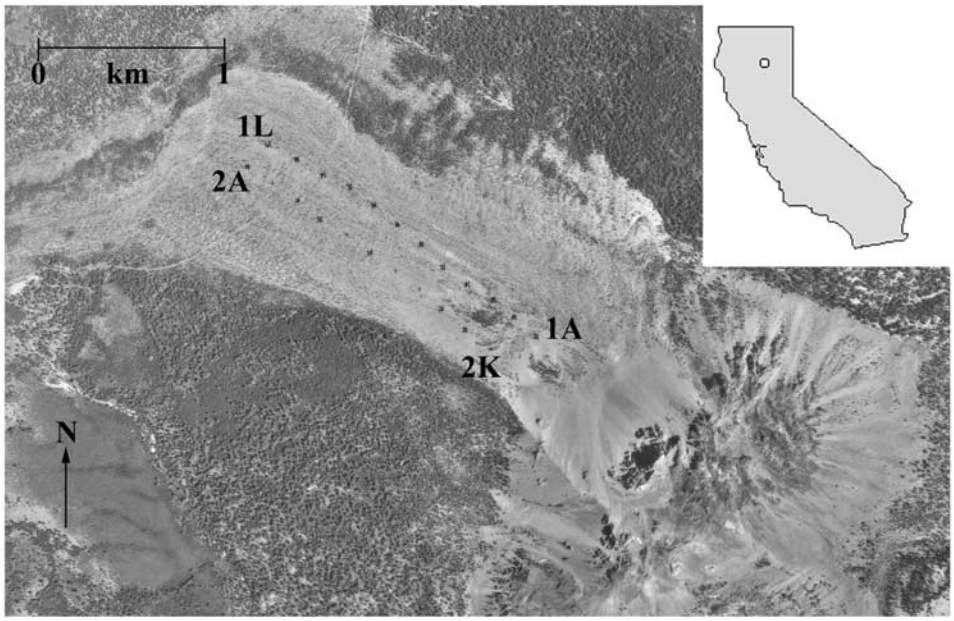

Figure 1. Georectified aerial photograph of the Chaos Jumbles rock avalanche, Lassen, California. Rock size measurement locations are indicated by pluses. Identifiers for measurement locations along bearing 1 are, from source to toe, 1A, 1B, 1C, 1D, 1E, 1F, 1G, 1H, 1I, 1J, 1K, and 1L. Identifiers for measurement locations along bearing 2 are, from toe to source, 2A, 2B, 2C, 2D, 2E, 2F, 2G, 2H, 2I, 2J, and 2K.

and Medicine Lake Volcano were collected by *Anderson et al.* [1998] are shown in Figure 3.

3. Field Approach

[13] The objective of this field study was to quantitatively characterize the surface block size distributions at each location. However, the actual block size distribution is something that is not easily defined for irregular clasts. Our approach is just one of many choices for estimating the actual distribution of block sizes on the surface. Even sieving measures only one dimension of each clast and is merely an estimate of the actual size distribution, with results sensitive to the amount of time each sample is shaken. Other methods characterize the angularity of clasts, or measure three orthogonal dimensions of each clast. However, few blocks on a lava flow or rock avalanche are box-shaped with well-defined axes. Thus determination of where to measure the various axes requires interpretation that can lead to nonunique results for each block. Even with three dimensions measured, one is still left with a variety of choices for how to combine these dimensions to arrive at a valid estimate of rock size. Often, the three-dimensional measurements are reduced to a single linear quantity, which by its very nature must be an estimate of rock size. The one-dimensional method described here does not require any interpretation in the field and leads to consistent, repeatable measurements. Here we demonstrate that our approach to estimating block size is effective for addressing the key objectives of this study.

[14] Locations for measurements of rocks along the Chaos Jumbles and lava flows at Sabancaya were selected along a cardinal bearing. This bearing was made with reference to a vertical air photo of the deposit and also corresponded to previously conducted topographic transects using differential GPS (dGPS) [*Bulmer and Campbell*, 1999; *Bulmer et al.*, 2002]. At selected locations along the cardinal bearing, two 20 m ropes were positioned perpendicular to each other with one rope parallel to the downslope movement direction. Along these rope lengths rock sizes were measured. The positions of end points for each rope length were recorded using a GPS Garmin 12 XL (<1 m accuracy in horizontal). The crossing points of the two orthogonal ropes at each rope length location along the cardinal bearing were spaced 150 m apart at the Jumbles and 250 m at Sabancaya.

[15] Measurements from 13 rope length sites were obtained along each of two transects that ran the length of the Jumbles deposit III (Figure 1). At each location (Figure 4), rocks were identified as being part of flow unit I, II, or III. At Sabancaya rock size measurements were made at 19 rope length sites (Figure 2) along transects that ran both along and across the flow 2a (Figure 5).

[16] All rocks and spaces directly under the two 20 m rope lengths at each site were measured on the Jumbles and flow 2a (Figure 6). In the lava flow and dome locations, no distinction was made between those blocks (or spines) that might still be connected to the flow interior and those blocks that are clearly broken pieces of the crust. Any blocks that are still connected to the flow interior are an important component of the surface block size distribution to be characterized statistically. Spaces occur between stacked rocks because of their irregular shape. The three descriptive criteria used to classify rock sizes along each rope length follow the convention of *Blair and McPhearson* [1999], >2 cm (very coarse pebble to block), <2 cm (coarse pebble to sand), and space (no rock). In instances where <2 cm rocks occurred under the rope the term fines was used and

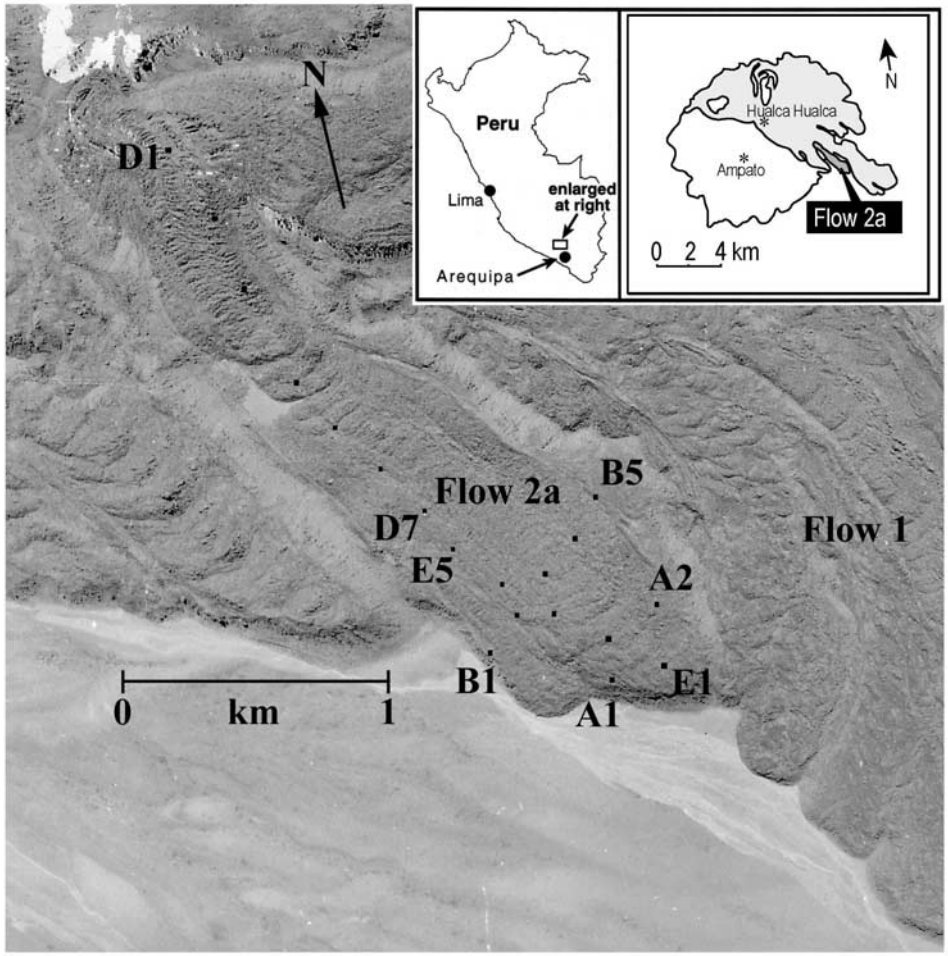

Figure 2. Georectified aerial photograph of Sabancaya, Peru. Rock size measurement locations on flow 2a are indicated by dots following dGPS transects from A1 to A2, B1 to B5, D1 to D7, and E1 to E5.

the collective distance to the next rock was measured rather than each individual small piece of rock. Following the rock measurement approach used by *Anderson et al.* [1998], only the dimension of each rock $\geq$2 cm under the rope was recorded. The diameter of the rope was smaller than our measurement cutoff of 2 cm. This is analogous to the method used to determine crystal size distributions in igneous rock thin sections where any one-dimensional measurement of size should give an average size distribution for the sample if the items are randomly oriented [*Cashman*, 1988; *Cashman and Marsh*, 1988]. There is very little ambiguity in this measurement approach. Simply, every rock lying directly beneath the rope is measured. As only the rock's dimension that lies along the rope is measured, this approach is substantially more time efficient than measuring the longest (L), intermediate (I), and shortest (S) dimensions for every rock along each transect. We show here that this technique gives a reasonable estimate of the average size distribution for the sample where the items are randomly oriented.

4. Statistical Analysis

[17] Throughout the analyses presented here, we have used inferential statistical procedures called analysis of variance (or ANOVA in the statistical literature [e.g., *Sheskin*, 1997]). ANOVA techniques are typically employed to evaluate the significance of differences between the mean values of more than two samples. A variety of ANOVA hypothesis tests can be called upon, including Fisher's least significant difference (LSD), Bonferroni-Dunn and Scheffé [*Sheskin*, 1997]. The confidence intervals generated by these tests for each sample mean take into account the reduced degrees of freedom resulting from the simultaneous estimation of means and standard deviations for multiple data sets. The overlap, or lack thereof, between confidence intervals can then be used to infer whether or not sample means are statistically the same or different.

[18] The magnitudes of the confidence intervals generated by each test vary somewhat because of constraints on the significance levels. In broad terms, Fisher's LSD intervals are the tightest (or smallest), Scheffé intervals are larger in magnitude, and Bonferroni intervals are generally somewhere between. By choosing LSD, there is a relatively higher risk of concluding two samples are different when in fact they are the same. With Scheffé there is a relatively higher risk of concluding two samples are the same when in fact they are different. Although our conclusions are not sensitive to the test used, we have based our conclusions on the intermediate Bonferroni intervals. For all

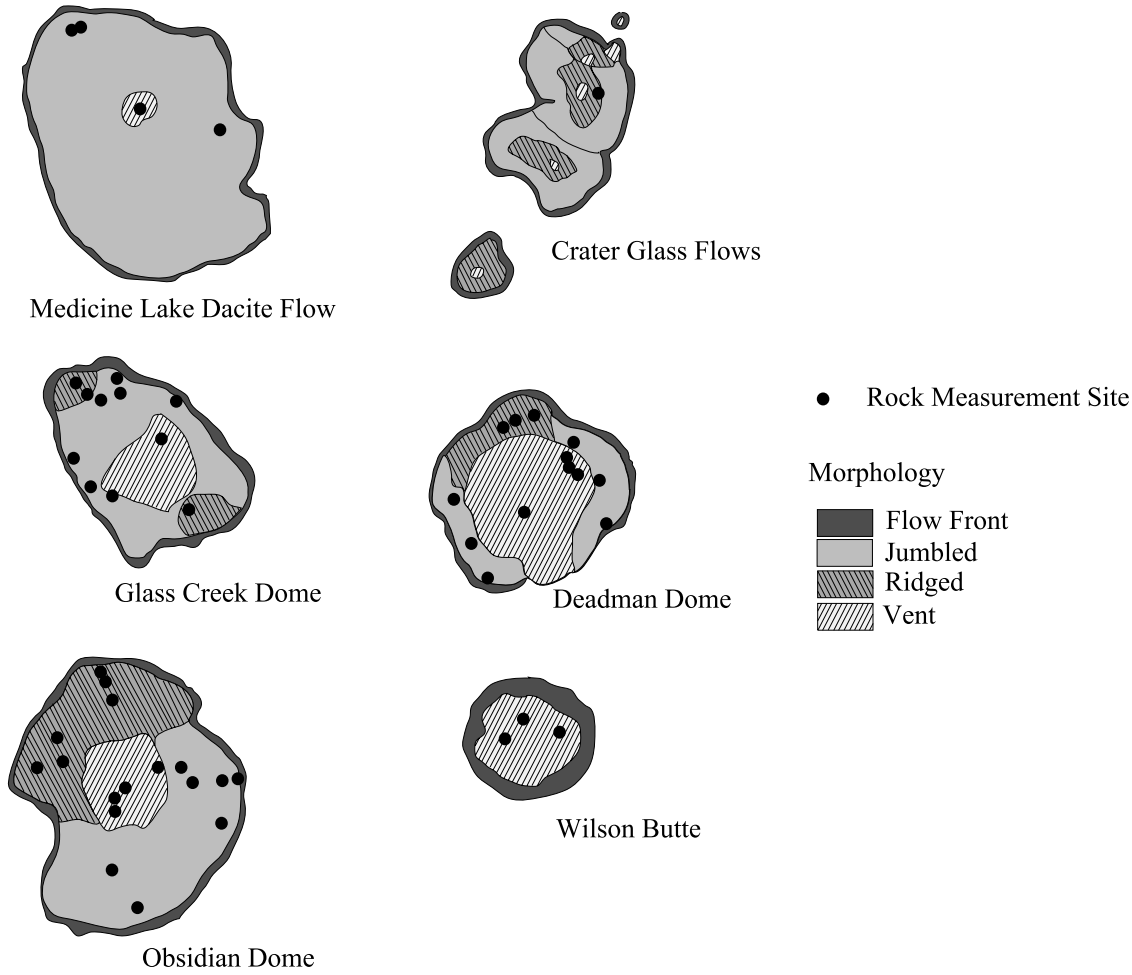

Figure 3. Cartoon showing the sites where rock size data were obtained on the Inyo domes and Medicine Lake Volcano from *Anderson et al.* [1998]. At each site, data were collected along orthogonal rope lengths on the flow surface.

tests, we have assumed a typical significance level of 5% (α = 0.05). The implication of this assumption is that there is a 5% probability of accepting our hypothesis when in fact it should be rejected. Here we state this significance level as 95% confidence intervals in the ANOVA discussions.

[19] All of the rock size sample distributions analyzed here are strongly skewed and are well described by a lognormal probability distribution. The lognormal distribution is often appropriate for asymmetric distributions of geologic data. Most standard hypothesis tests, however, assume that each sample is normally distributed (gaussian). Fortunately, we can easily transform the rock size data such that they are normal by taking the natural log. All ANOVA tests were performed on the transformed natural log of the rock sizes. Results were then transformed back to original units by exponentiation for presentation.

[20] Because of the broad range of rock sizes at the Jumbles, we were concerned that the larger rocks at each rope length site may have been undersampled by the rope length technique. To test for this, we defined a 2 m by 2 m control area at the center of the orthogonal rope lengths at location 1K (Figure 1). Within the control area, the L, I, and S dimensions of every rock on the top layer were measured. While this method was used to better characterize the larger rocks in the control area, smaller rocks may simultaneously be underrepresented primarily owing to the subjective nature of the term "top layer" and because smaller rocks are more likely to drop into spaces.

[21] For comparison with the rope length technique described in Section 3, we estimated the average dimension for each rock in the 2 m by 2 m control area from the relationship (L + I + S)/3. Figure 7 compares histograms for the two 20 m rope lengths with the 2 $\times$ 2 m control area at site 1K. In all three cases, we have taken the natural log of the rock "size". Visually, the histograms for the two rope lengths are very similar, while the histogram for the control area is slightly different. While the mean value of the histograms (Figures 7a and 7b) for the two 20 m rope lengths appears similar, the mean rock size within the control area (Figure 7c) is larger than either of the individual rope lengths. ANOVA supports this inference (Figure 7d). Using 95% Bonferroni intervals, the mean value of the transformed rock sizes for the two rope lengths are statistically indistinguishable, but both are significantly smaller than within the control area.

[22] However, because the control area sample has fewer smaller rocks, the mean value of rock sizes within the

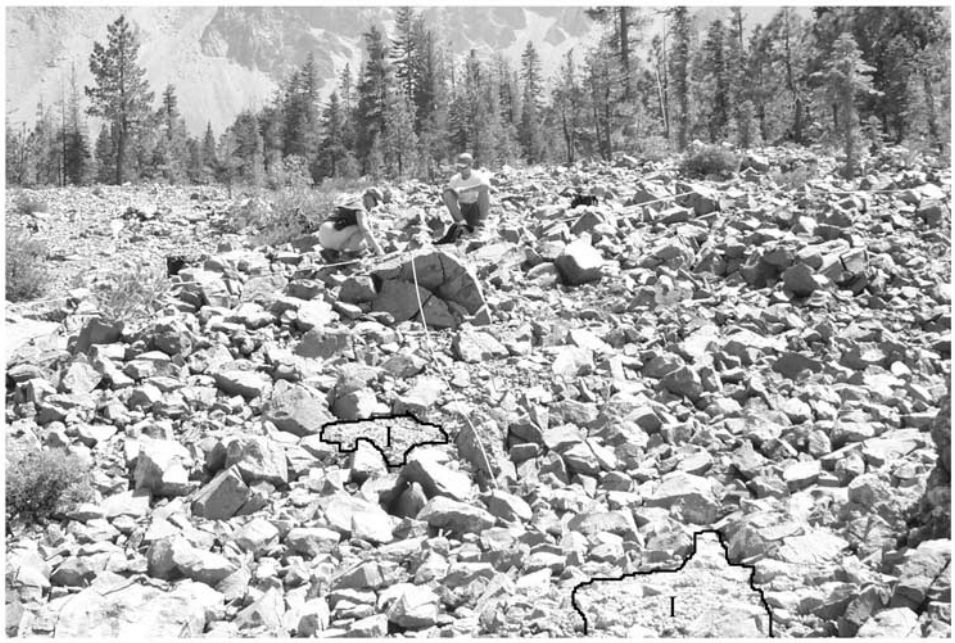

Figure 4. View up toward the Chaos Crags over avalanche deposits at site 1E. The two orthogonal rope lengths can be seen on the deposits. The rope oriented downslope crosses deposits from units III and I. Examples of unit I material are outlined and indicated by an I.

control area is increased relative to the two rope lengths. It is important to note that although the sample size is smaller, the distribution of larger rocks in the control area is similar to that found in the individual rope lengths. This gives us confidence that the rope length technique outlined by *Anderson et al.* [1998] is appropriate for the larger end of the rock size distribution, and is actually better than the averaging technique for characterizing the smaller rock sizes.

[23] We now demonstrate how surface rock size distributions collected at the Jumbles, Sabancaya, Inyo and Medicine Lake Volcano can be used to distinguish between their emplacement regimes (Figure 8). For this ANOVA analysis, we have combined rock size data for all samples from each deposit. This combination results in six pooled samples, one each for avalanche deposits I, II and III at the Jumbles, lava Flows 1 and 2a at Sabancaya, and all the silicic domes and flows at Inyo and Medicine Lake. For each sample, the arithmetic mean value and 95% Bonferroni intervals are determined using the transformed (natural log) rock sizes. When we take the exponent of the

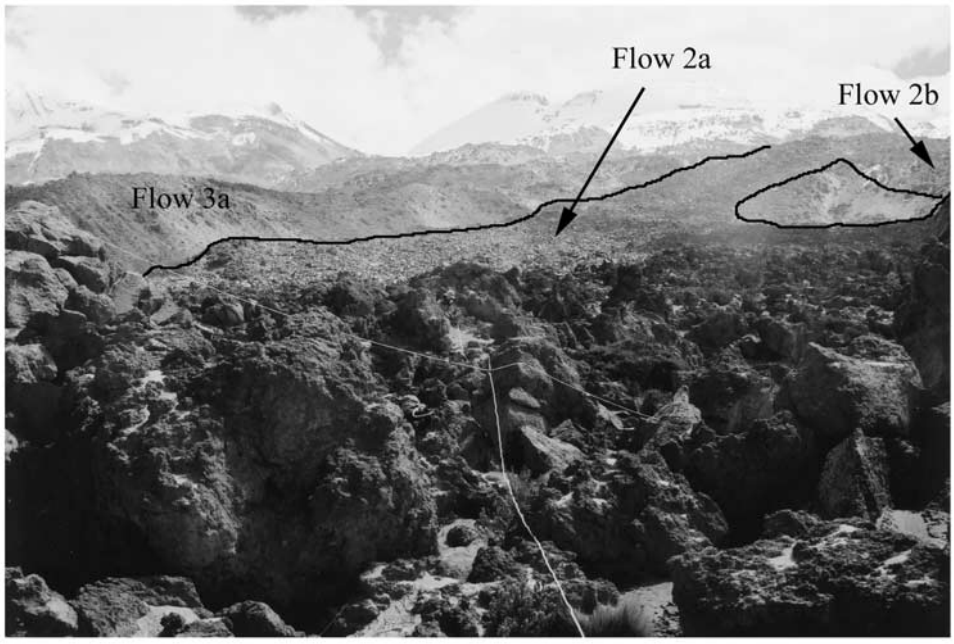

Figure 5. View up toward the Sabancaya source vent for flow 2a from site D7. The two orthogonal rope lengths can be seen on blocks on the flow.

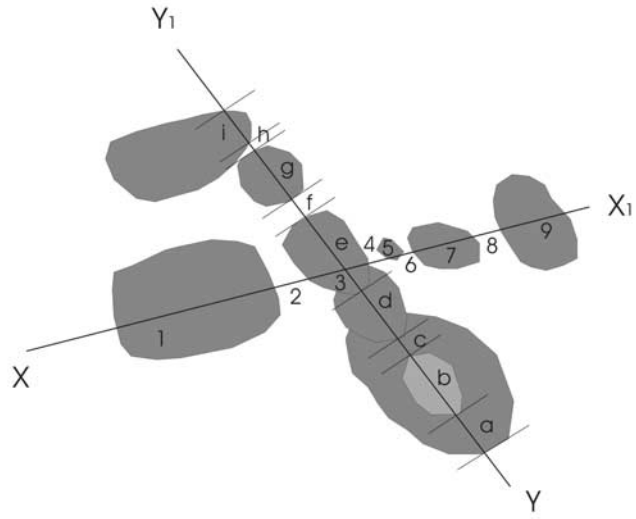

Figure 6. Lines X to X1 and Y to Y1 represent parts of the two 20 m rope lengths along which rock sizes were measured. For example, moving from Y to Y1, the first measurement along the rope length is from the edge of a to the leading edge of b. The second measurement is from the near edge of b to the far edge. The third measurement at c is the distance from the far edge of b to the near edge of d. The fourth measurement is the near edge of d to the near edge of e. The next is the near edge to the far edge of e. The next location f requires determination as to whether there is a void or a rock. If there is a space, then it is measured from the far edge of e to the near edge of g. At location i the measurement is made from the near to the far edge of i under the rope even though this can be seen to sample only a small part of the actual maximum rock size.

arithmetic mean value of the transformed data, the result is identically the geometric mean value of the untransformed rock sizes in original units. The geometric mean rock size is more appropriate for characterizing the location of the peak for these asymmetric rock size distributions with long tails. Thus Figure 8 shows the results of ANOVA comparing the geometric mean rock sizes for deposits from all three sites. Error bars correspond to the 95% Bonferroni intervals after the transformation has been reversed back to original units.

[24] From Figure 8, Jumbles deposit (I) has the smallest geometric mean rock size, and is distinct from any of the other deposits (i.e., Bonferroni intervals do not overlap with any others). Deposits II and III are indistinguishable from each other (based solely on rock size), but are significantly larger than deposit I and significantly smaller than the rocks found at the Inyo lava domes, Medicine Lake Volcano and at the Sabancaya flow. At Sabancaya, we find that the geometric mean rock sizes on the 1 and 2a flows are indistinguishable from each other, but significantly larger than all other deposits.

5. Discussion

[25] Two main inferences can be drawn from our analysis. The first is related to the rocky deposit as a whole and the second to the emplacement details for individual units making up a dome, lava flow or avalanche deposit. With reference to the first, Figure 8 shows that the size distributions of the surface deposits at the Jumbles, Sabancaya, Inyo and Medicine Lake Volcano are distinct and significantly different. Compositionally, the deposits at all locations are relatively similar. They are all silicic (andesite to dacite) volcanic deposits. They were, however, each emplaced by very different mechanisms. Thus the distinction between the surfaces we have examined may be used as a remote diagnostic tool to determine their emplacement origin. Additional information on rock size distributions for other deposits emplaced by similar mechanisms as those studied here would be very helpful in quantifying the amount of variability that exists within each category.

[26] The domes and lava flows at Inyo, Medicine Lake, and Sabancaya Volcanoes were all extrusive volcanic events. Thus new (primary) rocks (e.g., crust) were forming simultaneously as older (cooler) rocks were broken during emplacement. Conversely, the rock avalanches at the Jumbles were emplaced when existing domes with a primary rock population collapsed owing to mechanical failure. There is no evidence that these avalanches were hot (and certainly not molten) when they were emplaced. Thus there was no mechanism within the avalanche event for creating a primary rock population, only the ability to break up existing rocks forming a secondary rock population. In short, primary processes create the initial rock size populations. Secondary processes mobilize that population and can only modify the primary rock size distribution.

[27] It is also interesting that the Sabancaya, Inyo and Medicine Lake Volcano data are statistically different from each other. *Anderson et al.* [1998] suggest that primary rock size, for lava flows of similar composition, is a function of the rate of extrusion. This argues that the larger rocks at Sabancaya are the result of a relatively slower extrusion rate. However, this is at odds with the distance the flow traveled. Perhaps the best explanation for the long flow, large volume and large rocks is that the flow was hot and produced many new blocks during emplacement because of breakup of the crust.

[28] In addition to the ability to distinguish between geomorphic surfaces resulting from different emplacement processes, the second inference from our analysis is that we can use the data gathered from each rope length site to look for indicators of behavior within individual units. This in turn provides insight into the dynamics of the individual flow mechanisms. To demonstrate this, rock sizes measured along the two rope lengths at each site at Jumbles, Sabancaya, Inyo and Medicine Lake Volcano were combined and a geometric mean block size calculated.

5.1. Chaos Jumbles

[29] At the Chaos Jumbles we focused on the distribution of rock sizes both as a function of superposition (depositional unit) and distance from the source. Figure 9 shows the geometric mean rock sizes, and associated 95% Bonferroni intervals for samples from unit II as a function of distance along the deposit. For statistical reliance only rope lengths that have greater than 25 individual rock size measurements are shown.

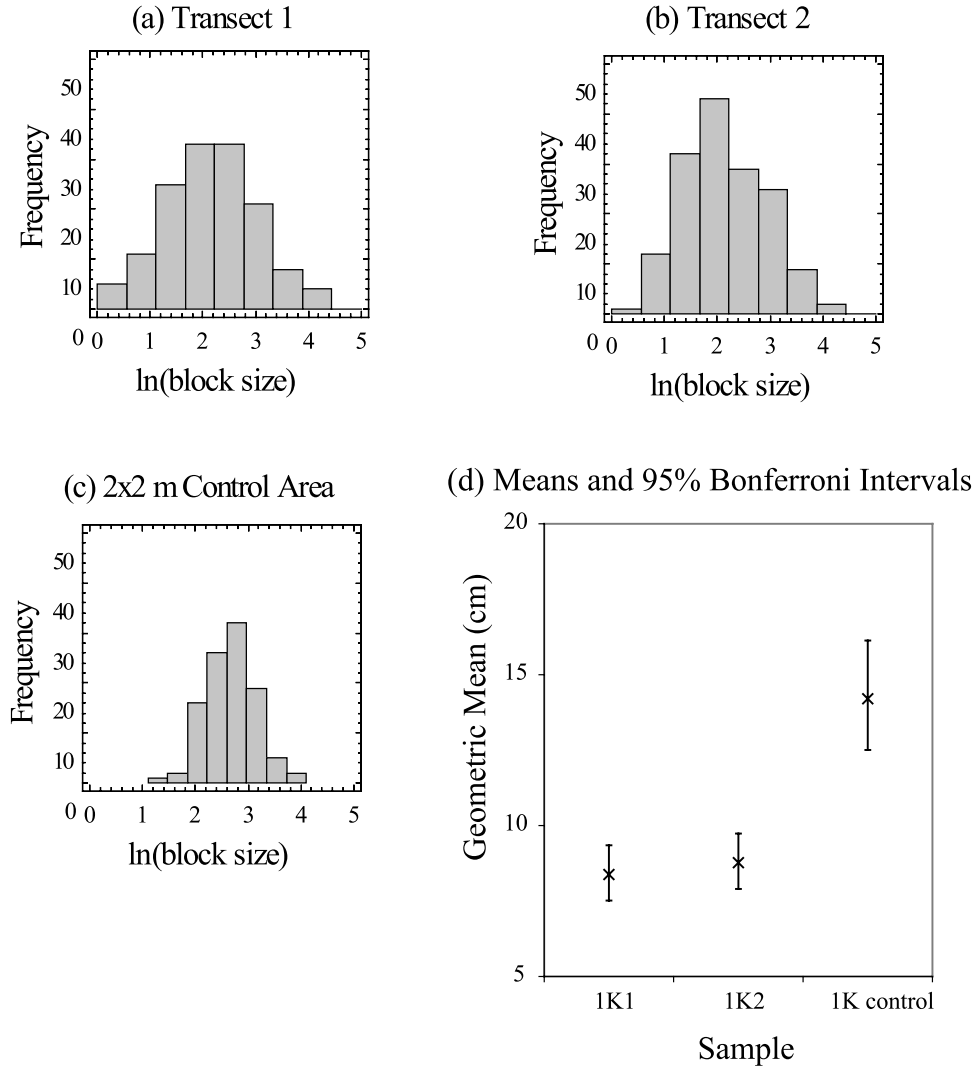

Figure 7. Empirical distributions for block sizes measured along (a) transect 1, (b) transect 2, and (c) 2 × 2 m control area, at Chaos Jumbles location 1K. All block sizes have been transformed by the natural log. (d) Comparison of the geometric mean block sizes at each location, along with associated 95% Bonferroni intervals.

[30] From Figure 9a we can see that the two rope length sites nearest the source (1A and 1B) have geometric mean rock sizes that are significantly larger than any of the other sites. To determine whether or not there is a significant trend as a function of distance we have looked for correlation between the geometric mean rock sizes at each location and distance of that location from the source. The correlation coefficient, r, can have values between −1 and +1, where zero indicates no correlation. The Pearson Product Moment correlation coefficient for the unit II blocks at the Jumbles is $r = -0.62$. The negative correlation coefficient for the Jumbles deposit indicates that block size decreases as distance increases. The hypothesis test for significance of the correlation coefficient is a two sided test [*Sheskin*, 1997]. The test determines if the correlation coefficient is significantly different from zero. At the 5% significance level, the critical value for 11 data points is 0.602. Because the calculated value of $|r|$ is greater than the critical value, we infer that the correlation is "significant" in statistical terms.

[31] In addition to rock size measurements made along the rope lengths at each site, we also measured the L, I and S dimensions of the largest rock within the 20 × 20 m area defined by the rope lengths. The decreasing trend in the geometric mean rock size observed along the deposit is confirmed upon analysis of the average dimension, $(L + I + S)/3$, of the biggest rocks. Again, considering only the Unit II samples, there is an even stronger negative correlation of $r = -0.86$ between the largest rock size and distance from the source. This correlation coefficient is greater than the critical value of 0.754 (for seven data points), thus we infer that the correlation is again significant.

[32] On the basis of these analyses we can infer that there is a general decrease in rock size as a function of distance for the Unit II deposit. This is consistent with an avalanche mechanism of rocks breaking up in transit because of mechanical stress as they move downslope.

[33] We have also explored the possibility of using ground-based photographs to measure rock size distributions. The ground-based photographs (such as that shown in

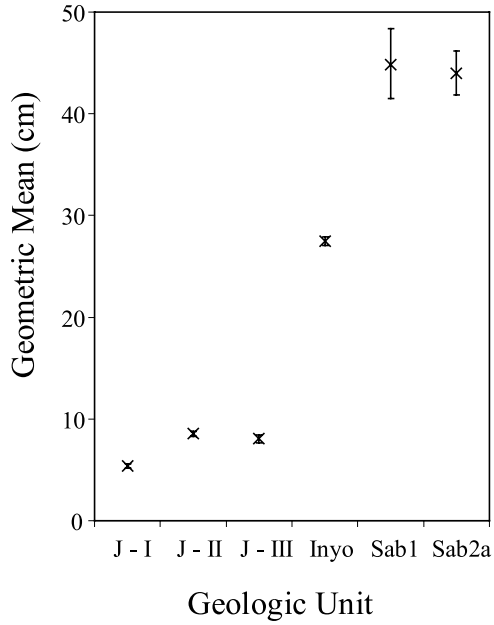

Figure 8. Geometric mean block size and 95% Bonferroni intervals for several volcanic units. Error bars for most points are smaller than the cross indicating the geometric mean. J-I, J-II, and J-III refer to the three flow units at Chaos Jumbles. Inyo refers to the silicic domes and flows at Inyo and Medicine Lake. Sab1 and Sab2a refer to the 1 and 2a lava flows at Sabancaya.

Figure 4) are analogous to those taken by the Mars Pathfinder and Mars Exploration Rovers (Spirit and Odyssey). Taking horizontal transects across a photograph of the 1F field site, rock sizes were measured in pixel units. The width of the measuring tape as it appears along this transect was used for scale.

[34] A total of 39 blocks (along two horizontal transects) were measured from the photograph at site 1F. The geometric mean block size using this method is 39.6 cm, compared to a geometric mean block size of 9.5 cm for site 1F from the field measurements. These two geometric mean values are statistically different (their error bars do not overlap), with the photograph measurements being systematically larger.

[35] Most of this discrepancy is a result of resolution differences. In the field, we are able to use a minimum block size of 2 cm, whereas the smallest blocks measured in the photograph are 5–10 cm. Small blocks are difficult to discern in comparison to shadow. In addition, the oblique angle of the photo also biases our measurements toward the larger clasts. Thus, while this technique is certainly valid and useable on photographic imagery (nadir or oblique), it is important to remember that the measured distribution is naturally deficient in smaller blocks.

[36] Although the mean value of block sizes measured from the photograph differs from that measured in the field, in absolute terms, the approach should work well on a relative basis when only remote image data are available. The technique can be used to compare different flows or to look for block size differences along a single flow.

5.2. Sabancaya Volcano

[37] For flow 2a at Sabancaya (Figure 2), rock size measurements were collected along rope lengths lying on dGPS transects running both parallel (profile D/E) and perpendicular (profile B) to the direction of flow. The flow contains lateral levees and flow-perpendicular surface ridges.

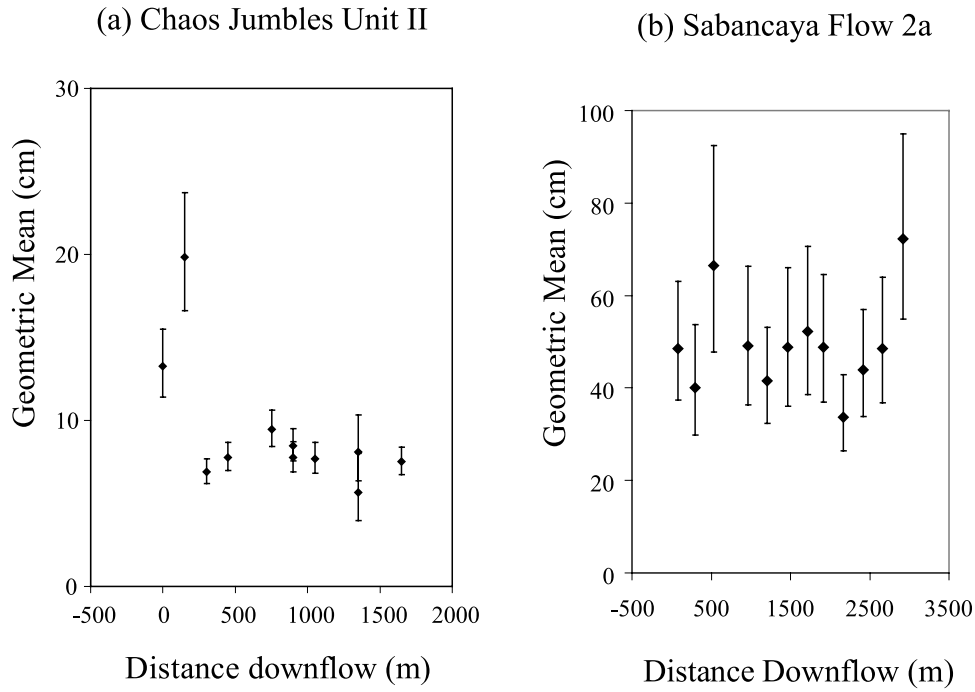

Figure 9. Geometric mean block sizes, as a function of distance along flow, with associated 95% Bonferroni intervals for (a) Chaos Jumbles unit II and (b) Sabancaya flow 2a.

[38] We looked for any differences in surface rock sizes in the cross flow direction of the 2a lava flow by comparing the geometric mean rock sizes at each rope length site along profile B. Using ANOVA, all of the 95% Bonferroni intervals around the geometric mean rock sizes show significant overlap with each other. We can therefore infer that there is no statistical difference in the geometric mean rock sizes along transect B. This indicates a coherent flow that is more or less homogeneous in the cross flow direction.

[39] For transect D/E (along flow, Figure 9b), the geometric mean rock sizes again appear relatively constant over a distance of approximately 2 km, possibly with somewhat larger rocks toward the flow front. To assess the possibility of an increasing trend in rock sizes, we again calculate the Pearson Product Moment correlation coefficient for the geometric mean rock size and distance from the source. The correlation coefficient $r = 0.13$, indicates a weak positive correlation. However, r is less than the critical value of 0.532 (for 12 data points), thus we infer that the correlation is not statistically significant.

[40] Note that many of the rope length sites at flow 2a contain one to three "megablocks" (on the order of 3, 5 or even 7 m in their longest dimension). Exclusion of these large blocks from our estimates of the geometric mean rock size at each location does not change our interpretation.

[41] Observations at the flow indicate that the rock size population is created by the extrusion of large slabs at the vent and the formation of crust along flow. Rocks can be modified through the formation of ridges or folds, breakage due to high mechanical stress, slope failures off the margins and weathering processes as noted by *Anderson et al.* [1998]. However, the production of the primary rock population offsets the rate at which rock sizes are modified resulting in the average block size population showing no change as a function of distance along the flow.

5.3. Inyo and Medicine Lake Volcano

[42] We can also use the detailed rock size measurements collected by *Anderson et al.* [1998] to make inferences regarding surface distribution of rocks for silicic domes and flows. The same methodology described above for collecting rock sizes was used at 67 locations at the Inyo dome complex (four domes) and three silicic flows at Medicine Lake Volcano. Using ANOVA to estimate 95% Bonferroni intervals, the geometric mean rock sizes at these sites were analyzed (Figure 10). There is significant overlap between the block size distributions for most of the 67 locations at Inyo and Medicine Lake (Figure 10a).

[43] *Anderson et al.* [1998] noted three distinct surface morphologies on the Inyo/Medicine Lake features; "ridged" areas contain prominent compressional ridges, vent areas show extreme topographic variations and spines, and jumbled areas show more subdued topography and appear to represent transitional areas between vent and ridged terrains. In Figure 10b, we have pooled block size data from 35 locations identified as ridged, 17 jumbled locations, and ten vent locations. We have then repeated the ANOVA for these three morphologic groups. On the basis of the 95% Bonferroni intervals, we see that vent and jumbled block sizes are statistically indistinguishable from each other, while the rock sizes measured in ridged terrain are significantly smaller than those in either vent or jumbled locations. Two important inferences can be drawn from this analysis. First, the block size distribution established at the vent locations appears to be preserved until ridge formation breaks the blocks. Second, despite independent classification of the jumbled locations based on morphology, the subtlety of the similarity with blocks in the vent areas and the difference from ridged areas, can only be distinguished through statistical analysis. This result has significant implications as regards future application of this approach to planetary sites, arguing for higher-resolution topographic data in order to identify these subtle differences.

[44] *Anderson et al.* [1998] suggested that lava flows that display decreasing rock size outward from the vent reflected gradually waning extrusion rates (high extrusion rates producing large strain rates and smaller blocks). Smaller rocks in ridged terrain reflect the more rapid extrusion and transport of vent rocks downslope accompanied by the fragmentation of rocks through thermal and mechanical processes. Glass Mountain, like the Sabancaya flow, shows no systematic change in rock size downslope. *Anderson et al.* [1998] found that long flows do not get smaller and smaller with respect to average rock size. New big rocks are added by compressional ridge formation and smaller rocks fall into "holes". At Sabancaya, we suggest that any decrease in rock size due to fragmentation is offset by the addition of larger rocks by breakage of crust at compressional ridges.

6. Conclusions

[45] Estimates of rock size populations for rock avalanches and lava flows have been obtained using standardized field techniques and statistically compared. Using ANOVA techniques and field observations it is possible to distinguish between primary (size making) and secondary (size modifying) emplacement populations based on rock size populations. This provides a methodology for improved remote geologic interpretation of the emplacement of blocky deposits. This technique could be used to improve geologic interpretations of the origin of a blocky surface in high-resolution image and topographic data when context is lacking, morphology is nonunique, and ground observations are not possible.

[46] In addition to the ability to distinguish between different emplacement processes, we can also use the data gathered from each rope length site to look for indicators of behavior within individual units. This in turn provides insight into the dynamics of the individual flow mechanisms. Variations in block sizes downslope occur in the rock avalanche rock population but are absent in the lava flows. Because the Jumbles were formed by a secondary emplacement process new blocks could not be formed. They could either remain unchanged from the original primary population or become smaller. In an avalanche, rocks are subject to high mechanical stresses that cause breakage and fragmentation. Evidence exists of percussion marks on rocks at the Jumbles indicating rock-to-rock strikes that suggest a high-energy state. This best explains the reduction in the average rock size as a function of distance along the avalanche for deposits II and III. Individual rock streams of deposits II and III can be identified by field observation and is supported by rock size analysis. These deposits remain uniformly one rock (10 cm) thick downslope and exhibit flow-like properties.

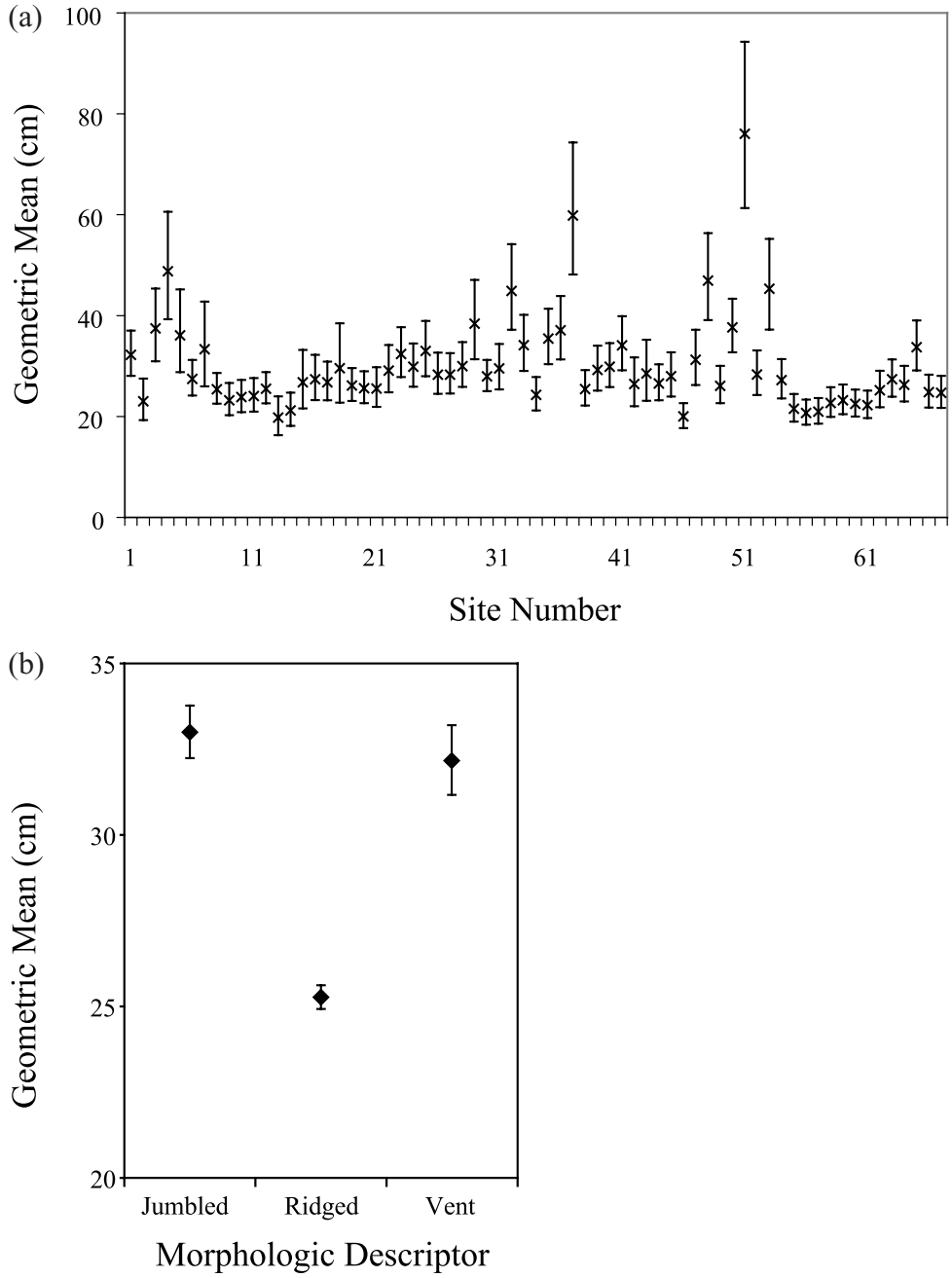

Figure 10. Geometric mean block sizes with associated 95% Bonferroni intervals for (a) each Inyo/Medicine Lake location identified by *Anderson et al.* [1998] and (b) Inyo/Medicine Lake data grouped by morphologic description (jumbled, ridged, or vent).

The sizes of unit I rocks identified in our transects over the area mapped as unit III by *Eppler et al.* [1987] may best be explained by weathering rather than mechanical stresses experienced either during its emplacement or caused by the subsequent events II and III. This is supported by examination of the toe of unit I which reveals the largest rocks (classified as blocks) in any of the Jumbles deposits. Because unit I is the oldest and most voluminous avalanche these blocks may be representative of the original rock sizes produced during dome formation and were preferentially carried to the front of the deposit. The emplacement mechanics of deposits II and III therefore appear to have been different from those of the larger volume unit I suggesting the importance of threshold dimensional values.

[47] At Sabancaya, Inyo, and Medicine Lake Volcano the blocks are produced from the extrusion of lava and the formation of crust. This rock population is then modified by secondary processes such as large-scale fold formation, breakage due to high mechanical stress, slope failures off the margins and weathering processes. However, the lack of systematic change in average block size downslope at Sabancaya and Glass Mountain flows suggest the rate of rock fragmentation is offset by the creation of large rocks during emplacement.

[48] This preliminary analysis is very encouraging for improving the interpretation of blocky deposits using either field data or high-resolution image data where available. Our results indicate that we can constrain the process of emplacement of a geologic surface as either being primary or secondary based on estimates of rock size. Future work should focus on exploring the influences on surface block size distributions resulting from variability in underlying slope, and exogenous versus endogenous growth in the case of domes. It would be very interesting to compare the results found here with additional data sets collected from other primary (e.g., impact cratering, moraines) and secondary (e.g., flooding and glacial) processes to constrain the degree of variability within each category.

[49] **Acknowledgments.** The authors thank O. Barnouin-Jha, W. Murphy, I. Turner, C. Goudy, N. Warner, and S. McColley for help with the collection of field data at Lassen and Sabancaya. We also thank N. Riggs, L. Keszthelyi, S. Calvari, and an anonymous associate editor for helpful and thoughtful reviews. Parts of this research were funded by the NASA MDAP program (NAG5-12271 and NAG5-11170).

References

Anderson, S. W., and J. H. Fink (1992), Crease structures; indicators of emplacement rates and surface stress regimes of lava flows, *Geol. Soc. Am. Bull.*, *104*, 615–625.

Anderson, S. W., J. H. Fink, and W. I. Rose (1995), Mount St. Helens and Santiaguito lava domes; the effect of short-term eruption rate on surface texture and degassing processes, *J. Volcanol. Geotherm. Res.*, *69*, 105–116.

Anderson, S. W., E. R. Stofan, J. J. Plaut, and D. A. Crown (1998), Block size distributions on silicic lava flow surfaces: Implications for emplacement conditions, *Geol. Soc. Am. Bull.*, *110*, 1258–1267.

Angeli, M. D., P. Gasparetto, R. M. Menotti, A. Pasuto, and M. Soldati (1998), Rock avalanches, in *Landslide Recognition: Identification, Movement and Causes*, edited by R. Dikau et al., pp. 190–201, John Wiley, Hoboken, N. J.

Bailey, R. A., G. B. Dalrymple, and M. A. Lanphere (1976), Volcanism, structure and geochronology of Long Valley caldera, Mono County, California, *J. Geophys. Res.*, *81*, 725–744.

Blair, T. C., and J. G. McPhearson (1999), Grain-size and textural classification of coarse sedimentary particles, *J. Sediment. Res.*, *69*, 6–19.

Bulmer, M. H., and B. A. Campbell (1999), Topographic data for a silicic lava flow: A planetary analog, *Lunar Planet. Sci. Conf.*, *XXX*, 1446–1447.

Bulmer, M. H., and J. E. Guest (1996), Modified volcanic domes and associated debris aprons on Venus, in *Volcano Instability on the Earth and Other Planets*, edited by W. J. McGuire, A. P. Jones, and J. Neuberg, *Geol. Soc. Spec. Publ.*, *110*, 349–371.

Bulmer, M. H., and J. B. Wilson (1999), Comparison of stellate volcanoes on Earth's seafloor with stellate domes on Venus using side scan sonar and Magellan synthetic aperture radar, *Earth Planet. Sci. Lett.*, *171*, 277–287.

Bulmer, M. H., F. C. Engle, and A. Johnston (1999), Analysis of Sabancaya volcano, southern Peru using RADARSAT and Landsat TM data, summary paper, 10 pp., RADARSAT ADRO Program, Can. Space Agency, Montreal, Ont., Canada.

Bulmer, M. H., B. A. Campbell, and J. Byrnes (2001), Field studies and radar remote sensing of silicic lava flows, *Lunar Planet Sci.*, *XXXII*, 1850.

Bulmer, M. H., L. Glaze, O. S. Barnouin-Jha, W. Murphy, and G. Neumann (2002), Modeling mass movements for planetary studies, *Lunar Planet. Sci Conf.*, *XXXIII*, 1533.

Cas, R. A. F., and J. V. Wright (1987), *Volcanic Successions, Modern and Ancient: A Geological Approach to Processes, Products and Successions*, 528 pp, Allen and Unwin, London.

Cashman, K. V. (1988), Crystallization of Mount St. Helens dacite: A quantitative textural approach, *Bull. Volcanol.*, *50*, 194–209.

Cashman, K. V., and B. D. Marsh (1988), Crystal size distribution in rocks and the kinetics and dynamics of crystallization: II. Makaopuhi lava lake, *Contrib. Mineral. Petrol.*, *99*, 292–305.

Clynne, M. A. (1999), A complex magma mixing origin for rocks erupted in 1915, Lassen Peak, California, *J. Petrol.*, *40*, 105–132.

Crandell, D. R., D. R. Mullineaux, R. S. Sigafoos, and M. Rubin (1974), Chaos Crags eruptions and rockfall-avalanches, Lassen Volcanic National Park, California, *J. Res. U.S. Geol. Surv.*, *2*, 49–59.

Eppler, D., J. Fink, and R. Fletcher (1987), Rheological properties of emplacement of the Chaos Jumbles rockfall avalanche, Lassen Volcanic National Park, California, *J. Geophys Res.*, *92*, 3623–3633.

Fink, J. H. (1983), Structure and emplacement of a rhyolitic obsidian flow: Little Glass Mountain, Medicine Lake Highland, northern California, *Geol. Soc. Am. Bull.*, *94*, 362–380.

Fink, J. H., and R. W. Griffiths (1990), Radial spreading of viscous-gravity currents with solidifying crust, *J. Fluid. Mech.*, *221*, 27–42.

Fink, J. H., and R. W. Griffiths (1992), A laboratory analog study of the surface morphology of lava flows extruded from point and line sources, *J. Volcanol. Geotherm. Res.*, *54*, 19–32.

Fink, J. H., and C. R. Manley (1987), Origin of pumiceous and glassy textures in rhyolite flows and domes, in *The Emplacement of Silicic Domes and Lava Flows*, edited by J. H. Fink, *Spec. Pap. Geol. Soc. Am.*, *212*, 77–88.

Fink, J. H., S. W. Anderson, and C. R. Manley (1992), Textural constraints on effusive silicic volcanism: Beyond the permeable foam model, *J. Geophys. Res.*, *97*, 9073–9083.

Folk, R. L., P. B. Andrews, and D. W. Lewis (1970), Detrital sedimentary rock classification and nomenclature for use in New Zealand, *N. Z. J. Geol. Geophys.*, *13*, 937–968.

Gaddis, L. R., P. J. Mouginis-Mark, and J. N. Hayashi (1990), Lava flow surface textures: SIR-B radar image texture, field observations, and terrain measurements, *Photogramm. Eng. Remote Sens.*, *2*, 211–224.

Golombek, M., and D. Rapp (1997), Size frequency distributions of rocks on Mars and Earth analog sites: Implications for future landed missions, *J. Geophys. Res.*, *102*, 4117–4130.

Heath, J. P. (1960), Repeated avalanches at Chaos Jumbles, Lassen Volcanic National Park, California, *Am. J. Sci.*, *258*, 744–751.

Malin, M. C. (1988), Rock populations as indicators of geologic process, in *Reports to Planetary Geology and Geophysics Program*, *NASA Tech Memo.*, *TM-4041*, 502–504.

Malin, M. C. (1989), Rock populations as indicators of geologic process, in *Reports to Planetary Geology and Geophysics Program*, *NASA Tech. Memo.*, *TM-4130*, 363–365.

Moore, H. J., J. J. Plaut, P. M. Schenk, and J. W. Head (1992), An unusual volcano on Venus, *J. Geophys. Res.*, *97*, 13,479–13,493.

Sheskin, D. J. (1997), *Handbook of Parametric and Nonparametric Statistical Procedures*, CRC Press, Boca Raton, Fla.

Stofan, E. R., S. W. Anderson, D. A. Crown, and J. J. Plaut (2000), Emplacement and composition of steep-sided domes on Venus, *J. Geophys. Res.*, *105*, 26,757–26,772.

Tanner, W. F. (1969), The particle size scale, *J. Sediment. Petrol.*, *39*, 809–812.

Udden, J. A. (1914), Mechanical composition of clastic sediments, *Geol. Soc. Am. Bull.*, *25*, 655–744.

Wentworth, C. K. (1922), A scale of grade and class terms for clastic sediments, *J. Geol.*, *30*, 377–392.

Wentworth, C. K. (1935), The terminology of coarse sediments, *Natl. Res. Counc. Bull.*, *98*, 225–246.

Williams, H. (1928), A recent volcanic eruption near Lassen Peak, California, *Univ. Calif. Publ. Geol. Sci.*, *17*, 241–263.

S. Anderson, Geology and Planetary Science Department, Black Hill State University, Spearfish, SD 57799-9102, USA.

M. H. Bulmer, JCET/UMBC, 1540 S. Rolling Road, Baltimore, MD 21227, USA. (mbulmer@jcet.umbc.edu)

L. S. Glaze and K. M. Shockey, Proxemy Research, 14300 Gallant Fox Lane, Suite 225, Bowie, MD 20715, USA. (lori@proxemy.com)